Developmental Biology **244,** 278–292 (2002)
doi:10.1006/dbio.2002.0585, available online at http://www.idealibrary.com on IDEAL®

in the Larva of an Ascidian, *Halocynthia roretzi*

Toshiaki Okada,*,[1] You Katsuyama,*,[2] Fumihito Ono,*,†,[3] and Yasushi Okamura‡,[4]

**Molecular Neurobiology Group, Neuroscience Research Institute, National Institute of Advanced Industrial Science and Technology (AIST), Tsukuba Central 6th, Higashi 1-1-1, Tsukuba, Ibaraki, 305-8566, Japan; †Department of Medical Physiology, Meiji College of Pharmacy, Kiyose, Tokyo 204-8588, Japan; and ‡Center for Integrative Bioscience, Okazaki National Research Institutes, Nishigonaka 38, Myodaiji, Okazaki, Aichi, 444-8585, Japan*

The generation of distinct classes of motor neurons underlies the development of complex motile behavior in all animals and is well characterized in chordates. Recent molecular studies indicate that the ascidian larval central nervous system (CNS) exhibits anteroposterior regionalization similar to that seen in the vertebrate CNS. To extend the understanding about the diversity of motor neurons in the ascidian larva, we have identified the number, position, and projection of individual motor neurons in *Halocynthia roretzi*, using a green fluorescent protein under the control of a neuron-specific promoter. Three pairs of motor neurons, each with a distinct shape and innervation pattern, were identified along the anteroposterior axis of the neural tube: the anterior and posterior pairs extend their axons toward dorsal muscle cells, whereas the middle pair project their axons toward ventral muscle. Overexpression of a dominant-negative form of a potassium channel in these cells resulted in paralysis on the injected side, thus these cells must constitute the major population of motor neurons responsible for swimming behavior. Lim class homeobox genes have been known as candidate genes that determine subtypes of motor neurons. Therefore, the expression pattern of *Hrlim*, which is a Lim class homeobox gene, was examined in the motor neuron precursors. All three motor neurons expressed *Hrlim* at the tailbud stage, although each down-regulated *Hrlim* at a different time. Misexpression of *Hrlim* in the epidermal lineage led to ectopic expression of *TuNa2*, a putative voltage-gated channel gene normally expressed predominantly in the three pairs of motor neurons. *Hrlim* may control membrane excitability of motor neurons by regulating ion channel gene expression.

Key Words: **neural tube; ion channel; dominant negative; swimming behavior; LIM homeodomain protein; tadpole larva; ascidian.**

INTRODUCTION

Early neural development of ascidian embryos is similar to the situation in vertebrates. In both systems, the neural plate rolls into a dorsal larval neural tube (Conklin, 1905; Nicol and Meinertzhagen, 1988a,b, 1991). The number of cells constituting the larval central nervous system (CNS) is, however, extremely small; in *Ciona intestinalis*, it is only about 370 cells, containing perhaps less than 100 neurons (Nicol and Meinertzhagen, 1991; reviewed in Meinertzhagen and Okamura, 2001). In addition, the cell lineages of ascidian CNS have been well studied using both morphological observations (Nicol and Meinertzhagen, 1988a,b) and injection of lineage tracers (Nishida and Satoh, 1985; Nishida, 1987). This simplicity of cellular organization and the detailed characterization of the invariable cell lineages of the ascidian CNS, together with the unique phylogenetic position of ascidians close to the ancestral origin of all chordate groups (Satoh, 1994; Swalla *et al.*, 1999), offers us a unique opportunity to gain insights into the acquisition of cellular diversity and complexity in the vertebrate nervous system during the course of chordate

[1] Present address: Howard Hughes Medical Institute and Department of Neurobiology & Behavior, State University of New York, Stony Brook, NY 11794.
[2] Present address: Department of Developmental and Cell Biology, University of California, Irvine, CA 92687.
[3] Present address: Department of Neurobiology & Behavior, State University of New York, Stony Brook, NY 11794.
[4] To whom correspondence should be addressed. Fax: +81-298-61-6551. E-mail: yokamura@nips.ac.jp.

0012-1606/02 $35.00

evolution. However, information regarding such basic features as the types of neurons and synaptic connections are all lacking, despite the simple organization of ascidians. This lack of information has been in part due to the lack of suitable molecular markers for individual neurons.

Using a voltage-gated sodium channel gene, *TuNa1* (Okamura *et al.*, 1994), as the first identified neuronal marker, we have previously shown that larval motor neurons, lying in the neural tube at the junction between the trunk and the tail, are derived from the embryonic blastomere called A5.2 in *Halocynthia roretzi* (Okada *et al.*, 1997) after the nomenclature of Conklin (1905). This origin of larval ascidian motor neurons shows several unique features during development, providing obvious contrasts with features of vertebrates. First, ascidian larval motor neurons originate from a blastomere that does not share a cell fate with epidermal cells, whereas the progeny of vertebrate neural plate cells have potential to develop into both neurons and epidermal cells. Second, the differentiation of ascidian larval motor neurons may not require tight cell contact; dissociated early blastomeres cultured in Ca-free sea water undergo neuronal differentiation (Okada *et al.*, 1997) as revealed by expression of two neuronal gene markers (Nagahora *et al.*, 2000; Y.O., unpublished data). This feature is not found in vertebrate motor neurons that differentiate by means of diffusible factors (Yamada *et al.*, 1993; Edlund and Jessell, 1999). Third, ascidian larval motor neurons are present only in the caudal neural tube at the proximal part of the tail (Bone, 1992; Nicol and Meinertzhagen, 1991; Okada *et al.*, 1997; Stanley-MacIsaac, 1999), while motor neurons of the vertebrate are distributed segmentally throughout the spinal cord. Previous studies of ascidians, however, lacked detailed information about individual larval motor neurons, which would be essential for further comparison with vertebrate motor neurons.

In an accompanying paper, we described the ascidian *synaptotagmin* (*syt*) gene, which is abundantly expressed in larval neurons (Katsuyama *et al.*, 2002). In this study, the promoter region of *syt* was used to drive the expression of green fluorescent protein (GFP) in developing *Halocynthia* motor neurons. By injecting the *syt* promoter–GFP reporter plasmid into a progenitor blastomere such as A5.2 or its direct precursor A4.1, three motor neurons with distinct morphology and innervation patterns were identified on each side of the neural tube. These motor neurons were arranged along the anterior–posterior (A-P) axis, reminiscent of the A-P segmental pattern in the vertebrate neural tube. The role of the ascidian LIM homolog, *Hrlim*, in determining individual motor neurons was also examined, because LIM homeodomain proteins determine motor neuron identity both in vertebrates (Tsuchida *et al.*, 1994) and the fruit fly (Thor *et al.*, 1999). We find that all precursors of the three motor neurons express *Hrlim* at the tailbud stage and that misexpressing *Hrlim* induces ectopic expression of a motor neuron-specific ion channel gene, *TuNa2*, in epidermal cells. These results implicate a regulatory role of the *Hrlim* protein in establishing membrane excitability that is unique to motor neurons.

MATERIALS AND METHODS

Animals

Adult ascidians, *H. roretzi*, were collected by fishermen in the northern parts of Japan, Wakkanai, and Sanriku. Animals were maintained at 6–8°C in circulating sea water. Spawning of eggs and sperm was induced by keeping the animals at 11°C under daylight. Eggs were collected in a nylon mesh having a mesh size of about 100 μm and were fertilized with sperm taken from another animal.

In Situ Hybridization

Each DIG-labeled RNA probe was synthesized from cDNA clones containing the full-length sequence of *Hrlim* and a partial sequence of *TuNa2* as described previously (Wada *et al.*, 1995; Nagahora *et al.*, 2000). A detailed protocol for the *in situ* hybridization has been reported previously (Okamura *et al.*, 1994; Okada *et al.*, 1997).

Plasmid Construction

The same plasmid employed for reporter gene analysis of *syt* was used to express GFP (Katsuyama *et al.*, 2002). A plasmid used in a previous study (Ono *et al.*, 1999) was utilized to drive the expression of DN-*TuKv2* in motor neurons. Briefly, a 3.4-kb-long sequence upstream of the ascidian *syt* gene (Katsuyama *et al.*, 2002) was fused to a mutated bright form of GFP, pEGFP-N1 (Clontech), and to a dominant negative form of *TuKv2* (Ono *et al.*, 1999) in pBluescript (Stratagene).

The plasmid containing the GFP-*Hrlim* fusion gene was made as follows. The coding region of *Hrlim* was amplified by using two primers: the sense primer (5′-AGATCTATGAATCTCATGTTCCATCAGGCGCGT-3′) and the antisense primer (5′-CTG CAG ATT AGC TGT TCC CGC ATT TCG-3′). Amplified PCR fragments were digested by *Bgl*II and *Pst*I and inserted into the multiple cloning site of GFP-C1 plasmid (Clontech). The GFP-*Hrlim* fusion gene was amplified by using the primers, the sense primer (5′-ACTAGTAGATCCGCTAGCGCTACCG-3′) and the antisense primer (5′-GAGCTCCCACAACTAGAATGCAGTGAA-3′). The sense primer corresponds to the sequence at the 5′ end of GFP and the Kozak consensus translation initiation site, which is located upstream of the GFP gene in the GFP plasmid. The antisense primer is targeted to the sequence located after the polyadenylation signals of the GFP plasmid. Amplified fragments were digested by *Spe*I and *Sac*I and were ligated to the downstream region of the *syt* promoter in pBluescript (Stratagene).

Plasmid Microinjection

Microinjection of plasmids into blastomeres was performed, with slight modifications, by a method described previously (Hirano and Nishida, 1997). Plasmids were injected manually by applying positive pressure with a glass micropipette penetrating the vitelline coat. Glass microcapillaries with a diameter of 1.0 mm were pulled with a programmable puller (Sutter Instruments) to a tip diameter of about 1 μm. Injected embryos were cultured on

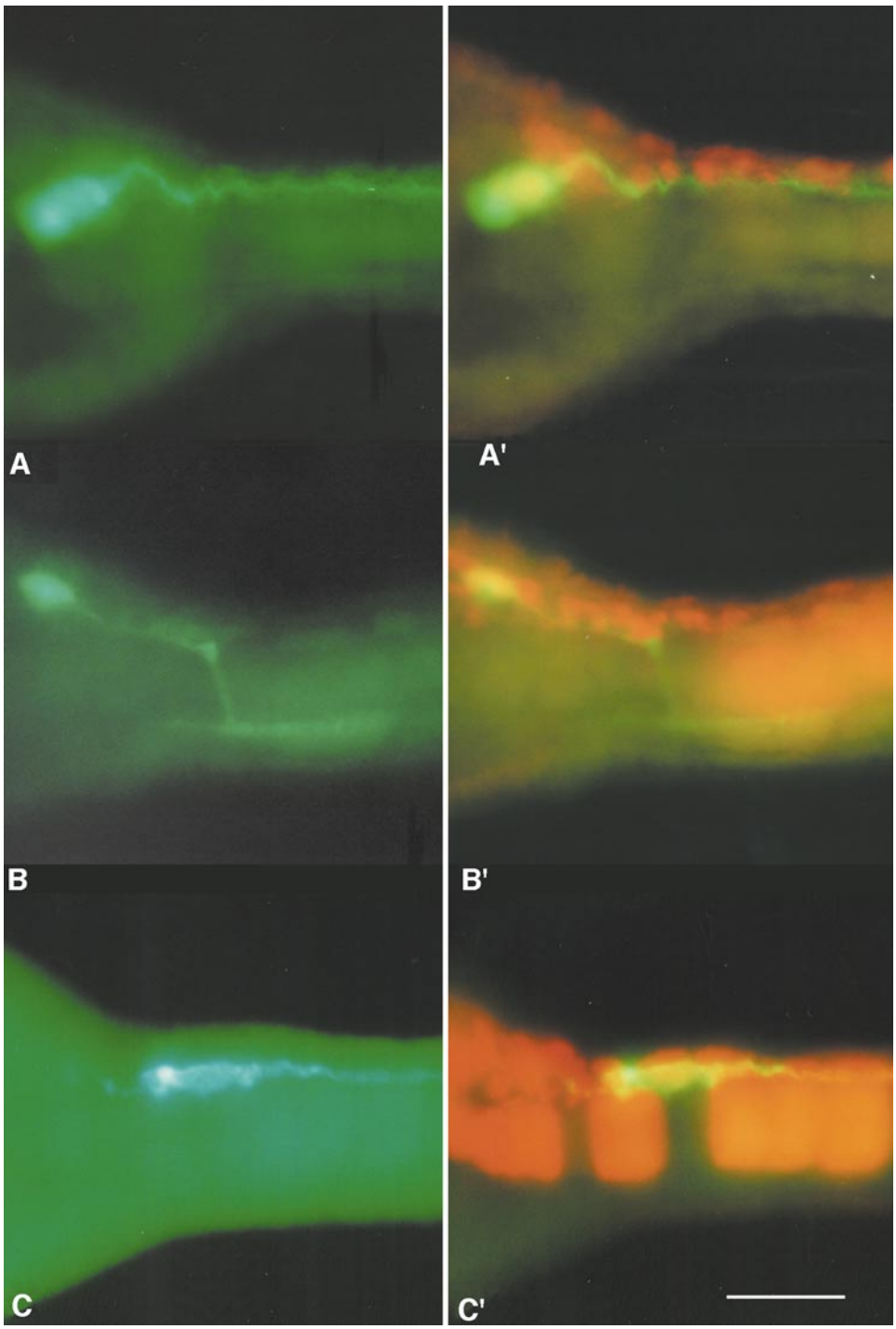

FIG. 1. Representative pictures of three individual motor neurons along the A-P axis. (A, A′) Moto-*a* has a single unbranched axon running along the dorsal muscle bands. Microinjection was performed in A5.2 blastomere at the 16-cell stage. (B, B′) Moto-*b* has an axon running toward the ventral muscles. The nerve endings are blanched and run along the ventral-most muscle cells. Microinjection was performed in A5.2 blastomere at the 16-cell stage. (C, C′) Moto-*c* has a long and narrow cell shape and a single, unbranched axon. Microinjection was performed in A4.1 blastomere at the eight-cell stage. GFP is visualized by its green fluorescence. Red signals originate from coinjected fast green. A GFP low pass filter was used in (A), (B), and (C), and a GFP band pass filter was used in (A′), (B′), and (C′). Scale bar, 50 μm.

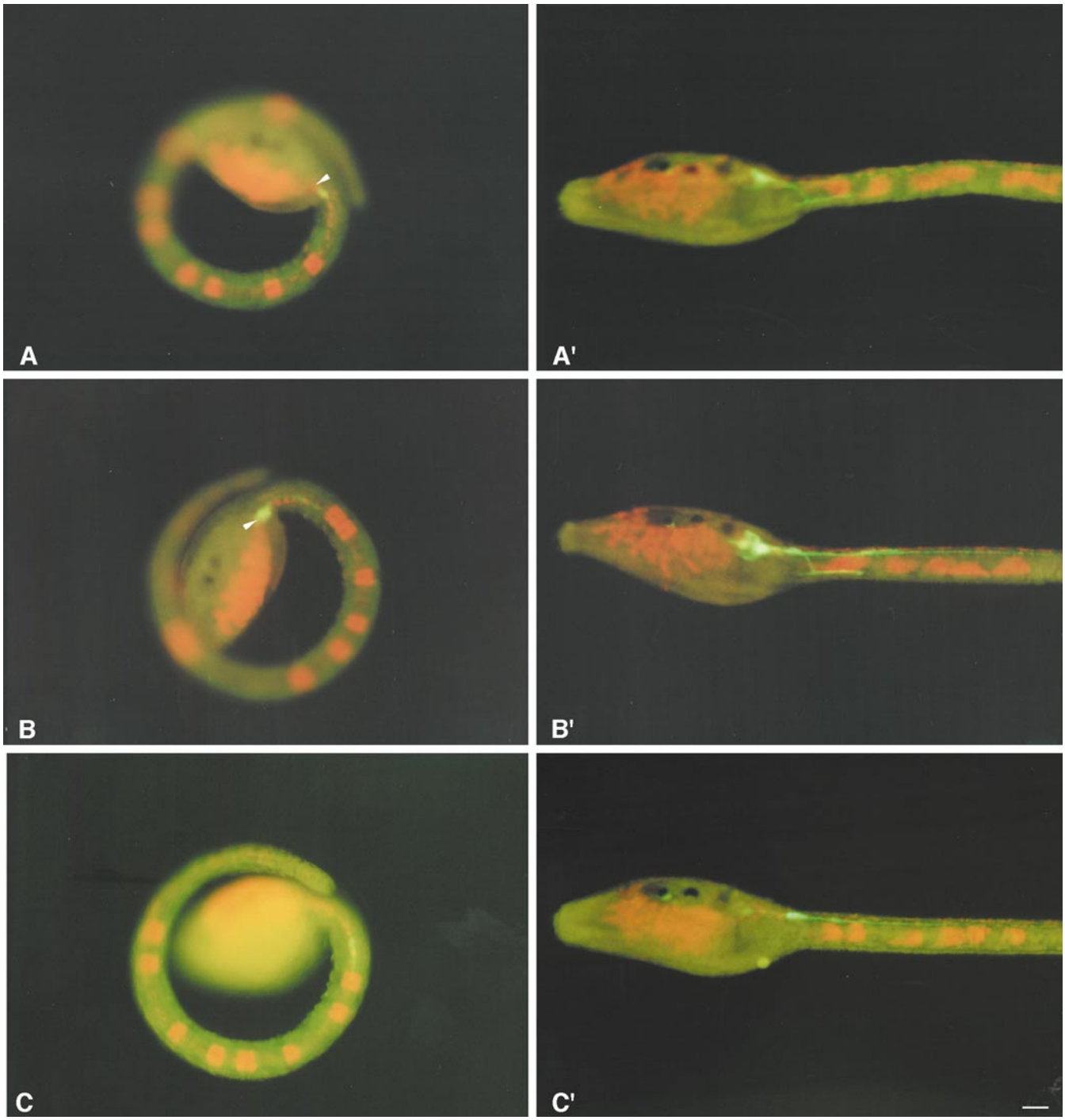

FIG. 2. Consecutive observation of individual motor neurons from young tadpole to larval stages. Animals shown in (A–C) developed into those in (A′–C′), respectively. All were microinjected at the 16-cell stage. (A, A′) A single cell, labeled by GFP, developed into Moto-*b*. Arrowhead indicates the anterior end of the A5.2-derived neural tube cells. (B, B′) Two labeled cells developed into Moto-*a* and Moto-*b*, respectively. Arrowhead indicates the anterior end corresponding to Moto-*a* precursor. (C, C′) One labeled cell with a posterior position developed into Moto-*c*. Scale bar, 50 μm.

agar-coated Petri dishes at 11°C until the appropriate embryonic or larval stage was reached.

For GFP expression in neurons, a solution containing 1–5 ng/μl GFP-plasmid and 0.2% fast green was used. Microinjection was performed into A4.1 at the 8-cell stage or into either A5.1 or A5.2 at the 16-cell stage.

For forced expression of the dominant negative (DN) form of a potassium channel (DN-*TuKv2*), a solution containing 10 ng/μl DN-*Tukv2*-plasmid, 5 ng/μl GFP-plasmid, and 0.2% fast green was injected into the A5.2 blastomere of the 16-cell-stage embryo. As a negative control, a solution containing only the GFP plasmid at 15 ng/μl was injected.

To misexpress *Hrlim* in epidermal cells, a solution of GFP-*Hrlim* fusion gene plasmid (10 ng/μl plasmid and 0.2% fast green) was microinjected into B3 of the four-cell-stage embryo or b4.2 of the eight-cell-stage embryo, which gives rise to epidermal progeny.

Epifluorescense Microscopic Observations

Injected larvae were observed with epifluorescence microscopy (Axiophot; Zeiss). Living specimens were treated with 10 mM tetraethylammonium, a potassium channel blocker that paralyzed the larva, and then were mounted on a glass slide in sea water containing 40% glycerol. Three kinds of emission filters were used: a conventional FITC filter, a GFP low pass filter (Chroma, #41015M, 485 nm), and a GFP band pass filter (Chroma, #41014, 510 ± 50 nm). When the GFP low pass filter was used, fast green (M.W. 808.86) showed a red signal. We found that a fast green signal was inherited only in descendants of an injected blastomere according to previously established lineage maps (Nishida and Satoh, 1985; Nishida, 1987). We were thus able to use fast green as a marker to trace the distribution of injected DNA in ascidian embryos. However, in some cases, GFP and fast green did not distribute equally in all cell progeny.

Laser Scanning Confocal Microscopy

To confirm the number of developing motor neurons, nuclei of embryos were stained with 0.003% propidium iodide (PI; Molecular Probes Inc.) in phosphate buffered saline (PBS) for 1 h at 25°C after *Hrlim* or *TuNa2* expression was detected by whole-mount *in situ* hybridization. Embryos were washed in PBS for 2–3 h and dehydrated in an ethanol series prior to clearing in benzylbenzoate/benzylalcohol (BB/BA). They were finally mounted in a silicone dish and examined by using confocal microscopy (Zeiss, LSM 510).

Double Staining with in Situ Hybridization and Anti-GFP Antibody

GFP-expressing larvae were fixed for *in situ* hybridization and stored in 70% ethanol at −20°C. We performed whole-mount *in situ* hybridization with the *Hrlim* probe or *TuNa2* probe, following the method described previously (Wada *et al.*, 1995; Okada *et al.*, 1997). After staining, the preparations were incubated with anti-GFP rabbit polyclonal antibody (1:200 in PBS; Molecular Probes, Inc.) for 5 h at 25°C. After washing in PBS, preparations were immersed in HRP-conjugated anti rabbit IgG antibody (1:50 in PBS; Dako) for 1 h at 25°C. HRP staining was performed by using 1 mg/ml diaminobenzidine with 0.003% H_2O_2 in 100 mM Tris (pH 7.5).

Analysis of Swimming Behavior

The swimming behavior of DN-*TuKv2*-injected and control larvae was studied in a Petri dish. Movement was recorded by using a digital high-speed CCD camera system (FASTCAM-Rabbit-mini; PHOTRON Limited) at 250 frames s^{-1}. Swimming of each larva was recorded for up to 5 min. Motions of swimming larva are available from our web site (http://www17.u-page.so-net.ne.jp/dc4/maboya/index2.html).

RESULTS

Three Pairs of Motor Neurons Show Distinct Morphological Characteristics

Using the Na^+ channel gene, *TuNa1*, as a molecular marker (Okamura *et al.*, 1994; Okada *et al.*, 1997), we previously showed that several motor neurons are present in the neural tube at the border between the trunk and the tail. We have recently cloned a *syt* gene from *Halocynthia* that is abundantly expressed in neurons of the entire larval nervous system (Katsuyama *et al.*, 2002). Although *in situ* hybridization using neuronal markers indicates the positions occupied by the somata of the neurons, detailed anatomical information about the individual neurons, their neurite projections or cell shapes in particular, cannot be obtained.

To identify the exact number, position, and axonal projection pattern of the motor neurons, we used the plasmid containing GFP downstream of the *syt* promoter. A 5′-upstream region of the *syt* gene, 3.4 kb in length, recently isolated from *Halocynthia*, drives gene expression in most neurons of the larval CNS (Katsuyama *et al.*, 2002). The plasmids were injected into blastomere A4.1 at the 8-cell stage or into its daughter, A5.2, at the 16-cell stage. These blastomeres have previously been shown to give rise to motor neurons in the neural tube at the trunk–tail border (Okada *et al.*, 1997). Following microinjection, GFP signals were examined at the larval stage by using epifluorescence microscopy. About 70% of injected larvae contained GFP-labeled cells in the neural tube at the trunk–tail border. Signals of *in situ* hybridization using the *syt* probe were also detected in the same region (Katsuyama *et al.*, 2002). Transgenic expression of GFP occurred in a mosaic manner, as previously reported (Hikosaka *et al.*, 1992). Thus, the number of GFP-positive cells varied from embryo to embryo. The number, however, was always between one and three, and in no case were there more than three cells, indicating that the A4.1 or its daughter, the A5.2 blastomere, gives rise to three motor neurons. All neurons on one side arose only from a single A5.2 blastomere. Migration of motor neurons across the midline was not observed, compatible with previous observations (Okada *et al.*, 1997).

Based on larvae that express GFP in one or two neurons in a mosaic manner, three types of neurons were identified and named as Moto-*a*, -*b*, and -*c*. Figure 1 shows typical examples of individual neurons. Moto-*a* extended a single, unbranched axon to the dorsal muscle band (Fig. 1A).

Moto-*a* was determined to be the most anterior of the three GFP-labeled cells by reference to the labeling inherited from coinjected fast green that exhibits orange color. The cell body of Moto-*a* was located around the anterior end of the caudal nerve cord derived from A5.2 (Fig. 1A′). Figure 1B shows the typical appearance of Moto-*b*. Moto-*b* extended its axon toward the ventral muscle band. The axon first ran dorsally along the proximal region of the neural tube, but then turned to the ventral side at about 50 μm from the cell body. As it reached the ventral muscle band, it branched into two axons: one axon running anteriorly and the other, posteriorly along ventral muscle. In some cases, more than two branches were found, but all ran in an anteroposterior direction. These branches appear to be identical to those producing synaptic terminals on ventral muscle cells previously shown by electron microscopy (Okada *et al.*, 1997). Judging from the labeling of coinjected fast green, this cell was not at the anterior end of the caudal nerve cord derived from A5.2, because a few cells labeled by the lineage tracer were located anterior to it (Fig. 1B′). Moto-*b* was thus positioned slightly posterior to Moto-*a*, although these two neurons often lay over one another along the dorsoventral axis (Fig. 2B′). Moto-*c*, the most posterior neuron, as judged from the labeling of coinjected fast green, had a uniquely elongate cell shape, thus making it easier to discriminate this neuron from the other two. Moto-*c* had a single unbranched axon that extended toward the dorsal muscle bands, similar to that of Moto-*a*.

To more clearly demonstrate the A-P order of Moto-*a* and -*b*, the development of each neuron was traced continuously from the young tadpole stage to swimming larva. Shown in Figs. 2A–2C are typical examples of the microinjected young tadpole embryos. Each of them grew up to the larva shown in Figs. 2A′–2C′. In Fig. 2A, the embryo has a single GFP-labeled cell. Based on the signals of coinjected fast green, this cell is not at the anterior end of the A5.2-derived neural tube. One or a few cells labeled by the lineage marker were located anterior to it. This GFP-positive cell differentiated into a Moto-*b* (Fig. 2A′). Figure 2B shows an embryo that had two GFP-labeled cells. These two cells aligned along the A-P axis. The anterior one seemed to correspond with the anterior end of lineage tracer signals in the neural tube. These two cells differentiated into Moto-*a* and -*b*, respectively (Fig. 2B′). These results are compatible with the idea that Moto-*a* is the most anterior cell of the neural tube derived from A5.2. A labeled cell positioned posterior to the cells shown in Figs. 2A and 2B developed into Moto-*c* (Figs. 2C and 2C′). This cell had a typical elongated shape already at the young tadpole stage. These results are consistent with the idea that precursors of Moto-*a*, -*b*, and -*c* align anterior to posterior at the young tadpole stage and that their relative positions do not significantly change from the young tadpole to the larval stage. In some cases, however, Moto-*a* and -*b* slightly changed their relative positions and became aligned next to each other in the dorsoventral direction. Notably, the positions of motor neuron precursors within embryos appear different from those in young tadpoles. At the young tadpole or larval stage, Moto-*a* and -*b* are located anterior to the border between the trunk and tail (for example, Fig. 2). At the tailbud stage, however, most anterior cells expressing neuronal markers are located in the tail, but not in the trunk (see Fig. 6). Probably cells forming the neural tube shift their relative positions to the trunk–tail border during late embryogenesis.

In some cases, GFP-labeled motor neurons showed neurites other than efferent axons, putatively dendrites, or possibly afferent axons. These neurites ran toward the pigment cells in the sensory vesicle (Figs. 3A and 3B). Unlike the efferent axons, such neurites were not always observed, probably because the GFP signal was too weak in these fine neurites. It is not yet clear whether these neurites are axonal or dendritic in nature.

We also addressed whether lineages other than A5.2 also give rise to motor neuron. When microinjections were performed in the A4.1 blastomere at the eight-cell stage, some GFP-labeled cells were found in the sensory vesicle (Figs. 3D and 3D′). We can predict that such neurons in the sensory vesicle would arise from the A5.1 blastomere that is derived from A4.1 as a sister cell of A5.2, because GFP-positive cells derived from A5.2 were confined only to the neural tube at the border between the trunk and tail. To test whether GFP-labeled cells found in the sensory vesicle of *Halocynthia* larvae included motor, the GFP-plasmid was microinjected into A5.1. A few GFP-labeled cells were consistently observed in the posterior region of the sensory vesicle, just below the pigment cells (Figs. 3C and 3D). These GFP-labeled cells derived from A5.1 extended their processes toward the region of the motor neurons (Figs. 3C and 3D), but never extended to the region of the muscle cells. Thus, rather than motor neurons, A5.1-derived cells in the sensory vesicle may be interneurons that innervate the motor neurons. We could not find any neurite extending to the tail muscle from neural cells derived from other blastomeres containing neural fate such as b4.2 and a4.2, a finding compatible with our previous study (Okada *et al.*, 1997). These findings suggest that the A5.2-derived neurons are the only population of motor neurons in *Halocynthia*.

Three Pairs of Motor Neurons Constitute the Major Functional Larval Motor Neurons

To confirm further that the three A5.2-derived pairs of neurons are the major functional group of motor neurons, we analyzed changes in the motile behavior of larvae by expressing a dominant negative form of a potassium (K^+) channel in Moto-*a*, -*b*, or -*c*. Recently, cDNA encoding a K^+ channel of the delayed-rectifier type, TuKv2, has been cloned from the *Halocynthia* larva and named *TuKv2* (Ono *et al.*, 1999). It was shown that overexpression of a dominant negative form of *TuKv2* (*DN-TuKv2*) abolished the endogenous neuronal delayed rectifier-type K^+ current, thus making action potentials longer than normal in neurons.

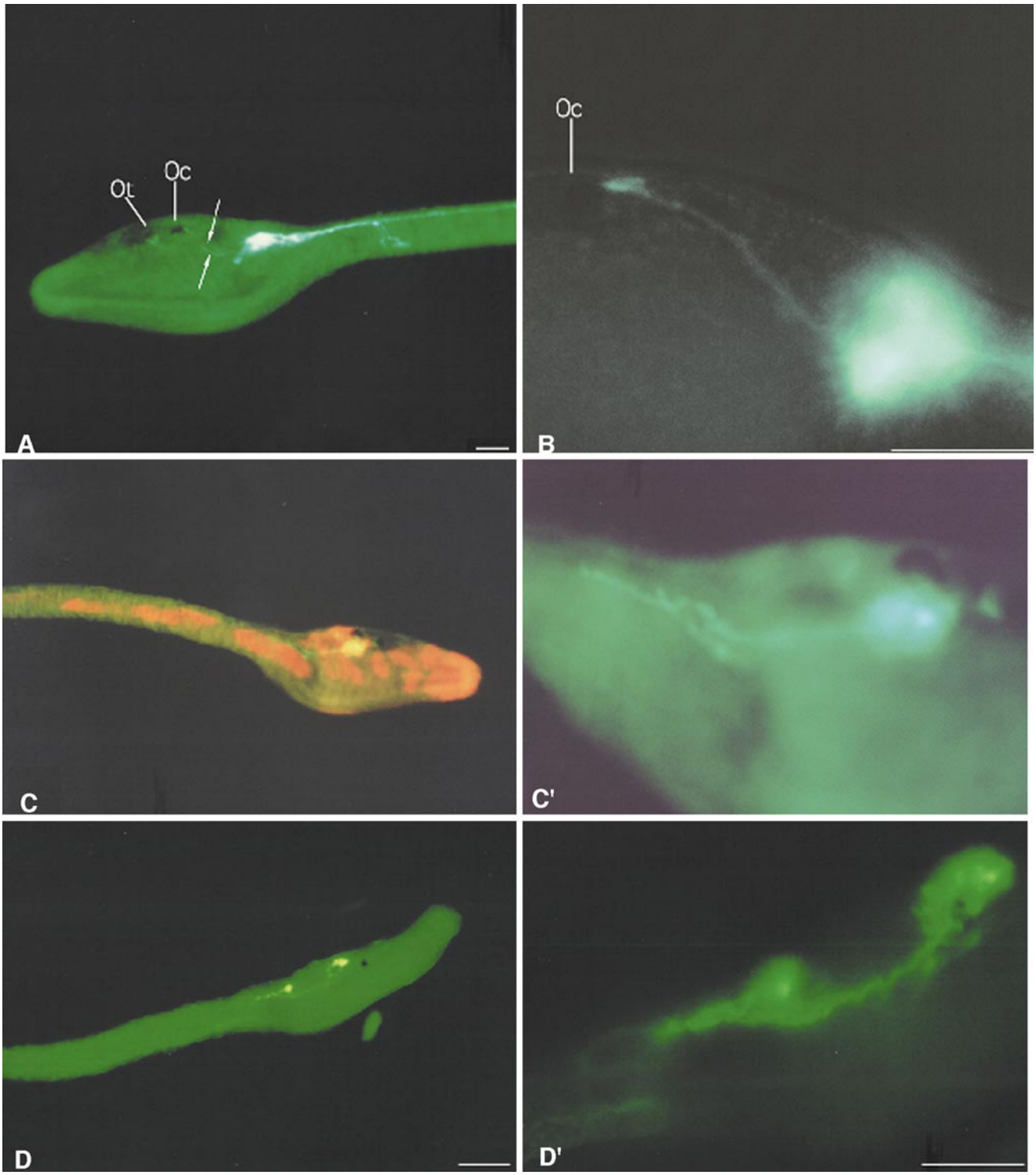

FIG. 3. (A, B) Putative dendrites or afferent neurites of A5.2-derived motor neurons visualized by the expression of GFP. (A) A few neurites (arrows) from motor neurons extending toward the sensory vesicle. Oc, ocellus; Ot, otolith. (B) Magnified view of (A). Single fibers (arrow) originating from Moto-*a* or Moto-*b* appear to extend toward the ocellus (Oc). Scale bar, 50 μm. (C, C′, D, D′) Larva in which GFP is expressed in A5.1-derived neurons. (C) The GFP plasmid was microinjected into A5.1 at the 16-cell stage. GFP-labeled cells were observed only in the sensory vesicle. Neurites stop anterior to muscle bands, suggesting that motor neurons are not derived from A5.1. (C′) Magnified view of (C). (D) Microinjection of GFP plasmid was performed in A4.1 at the 8-cell stage. In addition to neurons in the sensory vesicle just posterior to the pigment cell, Moto-*b* was labeled as judged from its typical ventral projection and the location of the somata. (D′) Magnified view of (D) shows cell bodies of neurons close to the sensory vesicle (right side) and Moto-*b* (left side). The neurons close to the sensory vesicle extend axons just posterior to Moto-*b*, possibly onto Moto-*c*, which was not labeled in this sample due to mosaic transgene expression. Red signals originated from coinjected fast green. C, D and C′, D′ are shown at the same scale (scale bar, 50 μm), respectively.

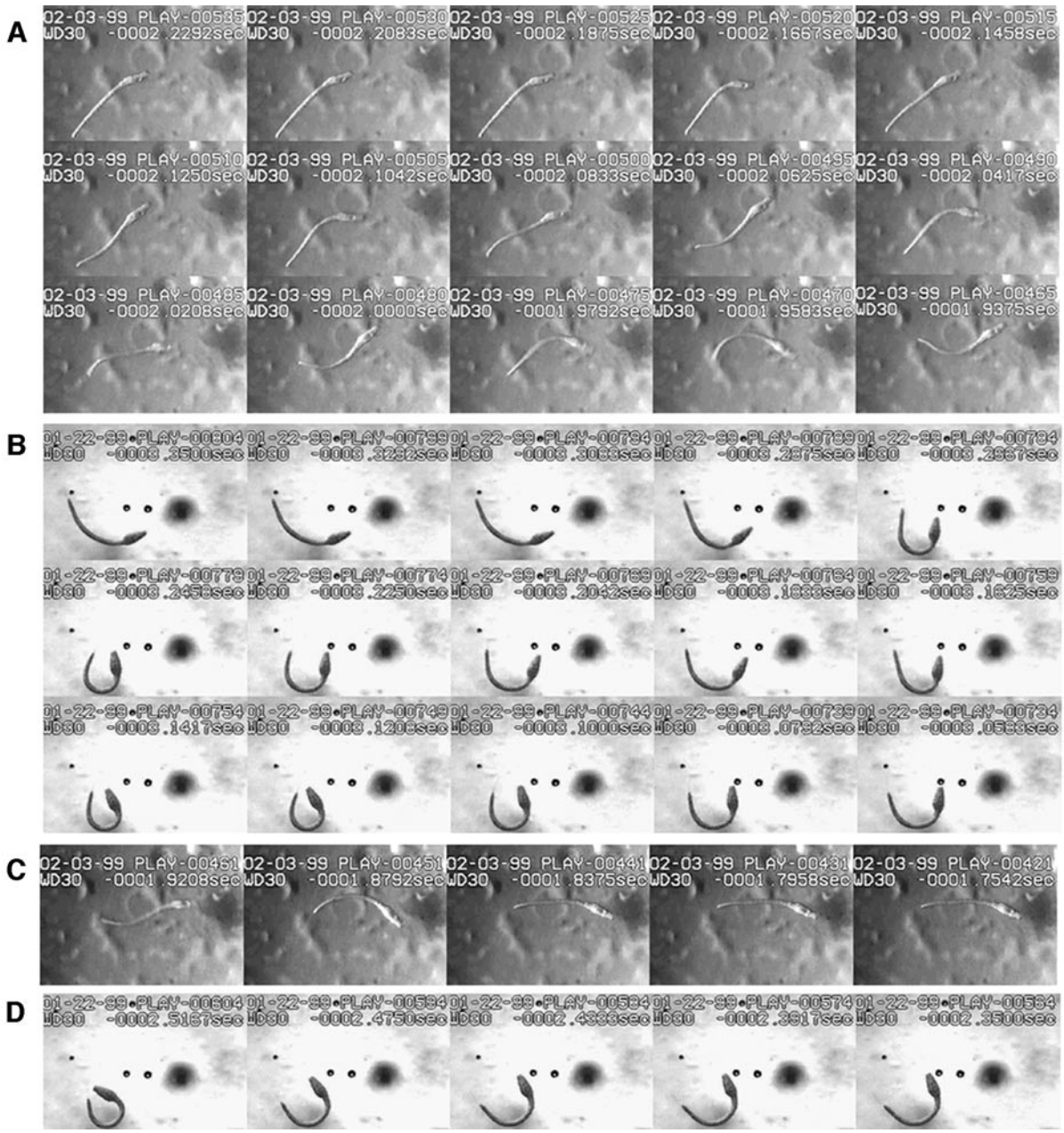

FIG. 4. Perturbation of swimming behavior by expression of a dominant negative form of the K^+ channel. Swimming behavior was compared between a normal larva and a larva expressing the dominant negative form of the potassium channel selectively in the A5.2 lineage. (A) Control larva that was injected with the GFP plasmid at the 16-cell stage. The larva bends its tail to either side and swims forward. Four cycles of the tail waves are completed in about 65 frames. (B) A larva expressing dominant negative K^+ channel in neurons derived from A5.2 blastomere. The larva bends its tail only to one side and cannot swim forward. Two cycles of bending are completed in about 50 frames. (C) Resting posture of the same control larva as in (A) after an episode of bending. The tail returns rapidly to the same posture prior to swimming (see first three frames in A). (D) Resting posture of the DN-injected larva shown in (B). The tail curves like a bow. Compared with the resting posture before one-sided bendings (see first three frames in B), the tail curves more markedly. Video images were recorded at 250 frames per second. Each frame was collected at 5-frame intervals in (A) and (B) and at 10-frame intervals in (C) and (D).

The plasmid containing the *DN-TuKv2* cDNA downstream of ascidian *synaptotagmin* and GFP plasmid were coinjected into A5.2 blastomeres. The injected embryos were allowed to develop to the larval stage, when their swimming patterns were examined. The GFP plasmid was coinjected to facilitate selection of those embryos express-

ing *DN-TuKv2* in motor neurons. Figure 4A shows the swimming behavior of a control larva (which express only GFP) recorded using a digital high-speed camera at 250 frames s^{-1}. Such control larvae could swim forward by rhythmically and symmetrically bending their tails (n = 34/39; 87%). By contrast, up to 50% (11/22) of larvae expressing the dominant negative K^+ channel (designated as "*DN*-injected") could not swim forward. In the most extreme cases (n = 3), DN-injected larvae bent their tail only to the intact side with normal rhythmic contractions, but failed to show any twitch or movement episode on the injected side during 5 min of observation (Fig. 4B). In less severe cases (n = 8), larvae showed some movements on the injected side. In these larvae, however, the frequency of flexions on the injected side was less than that on the intact side, and the amplitude of tail inflection on the injected side was also smaller. Another remarkable difference in *DN*-injected larvae was a curved posture in the resting state. In control larvae, the tail was stretched out almost straight at rest (for example, the first three frames shown in Fig. 4A). In contrast, tails of *DN*-injected larvae were often curved even at rest (the first three frames shown in Fig. 4B). In particular, the abnormality of the resting posture of *DN*-injected larvae became more remarkable just after episodes of twitching (Figs. 4C and 4D). In Fig. 4B, the tail of the injected side (right side of larva) seemed to be relaxed. After one-sided bending episodes, the tails of such larvae were curved more markedly than before episodes of movement (Fig. 4D). Such paralysis and the curved resting posture of *DN*-injected larvae appear to be caused by abnormal electrical properties of motor neurons of the injected side; control injection of GFP plasmids failed, in most cases, to cause abnormal swimming patterns. These findings support the view that A5.2-derived motor neurons are the major functional motor neurons for larval swimming.

Identification of Precursors of Three Pairs of Motor Neurons at the Tailbud Stage

We next explored earlier developmental aspects of the three pairs of motor neurons. The *syt* promoter did not drive gene expression early enough to detect a GFP signal before the young tadpole stage. Therefore, in order to trace motor neuron differentiation prior to the young tadpole stage, we marked the developing motor neurons by using *TuNa2*, a putative voltage-gated sodium channel gene, which is expressed in several lateral cells of the neural tube around the trunk–tail border. Transcription of *TuNa2* starts before the young tadpole stage (Nagahora *et al.*, 2000). We first examined whether these *TuNa2*-positive neurons at the young tadpole stage are motor neurons. The GFP plasmid was introduced into the A5.2 blastomere, and hatched larvae were processed for *in situ* hybridization with a *TuNa2* probe. Motor neurons that contained GFP protein were then visualized by immunostaining with an antibody against GFP. Since GFP was expressed in a mosaic manner, we needed to collect multiple specimens to determine which of the three motor neurons expressed *TuNa2*. Figure 5 demonstrates individual cases in which each of Moto-*a*, -*b*, and -*c* was double-labeled with GFP immunostaining and *TuNa2* signals. By combining multiple specimens, it was concluded that all three types of motor neurons expressed *TuNa2* and that no other cell expressed *TuNa2* in this region. Therefore, *TuNa2* serves as a reliable gene marker for motor neurons.

To identify earlier cell lineages for the three pairs of motor neurons, whole-mount *in situ* hybridization of tailbud embryos was performed with *TuNa2* probe. In the early tailbud, only two pairs of *TuNa2*-positive spots were observed in the neural tube (Fig. 6A). To resolve these spots into constituent cells and to define the exact number and location of *TuNa2*-positive cells, nuclei of embryos were stained with PI following whole-mount *in situ* hybridization for *TuNa2*. Serial optical sections were collected by confocal laser microscopy. Although the *in situ* hybridization signals masked the PI signal for cell nuclei, the dye for the *in situ* hybridization signal by *TuNa2* tended to fade with time in BB/BA solution. This fading made it possible to locate the *in situ* hybridization signal in a specific cell nucleus by continuous observation. It was found that, at the early tailbud stage, the anterior spot of each side in the whole-mount embryo consisted of two *TuNa2*-positive cells, and the posterior spot consisted of only one cell (Figs. 6B and 6C). The cells in the anterior spot were small and flat. On the other hand, the cell in the posterior spot had a large volume and nearly oval shape and was positioned slightly ventral to others in the neural tube. Anterior and posterior spots were spaced by at least one *TuNa2*-negative cell. From the number of *TuNa2*-positive cells and the continuity of gene expression patterns between the tailbud and tadpole stages, we concluded that three *TuNa2*-positive cells in anteroposterior sequence were precursors of Moto-*a*, -*b*, and -*c*, respectively.

Hrlim Is Expressed in All Precursors of Motor Neurons

In the vertebrate spinal cord, the exact combination of LIM-homeodomain proteins determines the subtypes of motor neurons (Tsuchida *et al.*, 1994). In the ascidian larva, *Hrlim*, a LIM class homeobox gene, has recently been identified (Wada *et al.*, 1995). *Hrlim* is expressed in the neural tube at the early tailbud stage and is detected as two pairs of signals (Wada *et al.*, 1995), a feature which is reminiscent of the two pairs of *TuNa2*-positive spots in our study.

To establish whether *Hrlim* is expressed in motor neuron precursors, the exact position of cells expressing *Hrlim* was defined by PI staining following *in situ* hybridization as described above. In the early tailbud stage, two pairs of *Hrlim*-positive spots were observed in the neural tube (Fig. 6D). At this stage, the anterior spot of each side in the

whole-mount embryo consisted of two *Hrlim*-positive cells and the posterior spot consisted of only one cell (Figs. 6E and 6F), as in the case of *TuNa2*-positive spots. Confocal microscopic observations showed that the number, position, and cell shape of *Hrlim*-positive cells were identical to those of *TuNa2*-positive cells (Figs. 6B and 6C). This indicates that *Hrlim* is expressed in precursors of Moto-*a*, -*b*, and -*c*. The posterior signals corresponding to the Moto-*c* precursor disappeared by the midtailbud stage (Fig. 6G), so that only two cells retained *Hrlim* expression (Figs. 6H and 6I).

Hrlim expression of identified motor neurons was also examined at the larval stage by the double-staining method with GFP-immunostaining and *in situ* hybridization. Moto-*a* was labeled by *Hrlim* signal (Fig. 7A, left), whereas Moto-*b* and Moto-*c* were not (Fig. 7A, right), indicating that *Hrlim* signal is down-regulated in Moto-*b* before the larval stage. In summary, *Hrlim* is initially expressed in all precursors of motor neurons at the tailbud stage and is subsequently down-regulated in two, first in Moto-*c*, then in Moto-*b*.

Ion Channel Gene Expression Is Induced Ectopically by Misexpression of Hrlim

The above results showed that *Hrlim* expression was detected in all precursors of three pairs of motor neurons, but was differentially regulated in the three types of motor neurons at subsequent developmental stages. This finding raises the possibility that *Hrlim* plays a role in determining the characteristic projection patterns of these motor neurons. Therefore, truncated *Hrlim*, lacking the homeodomain and potentially working as a dominant negative protein (Kikuchi *et al.*, 1997), was forced to be overexpressed in all three motor neurons by using the *syt* promoter. However, it did not lead to any change in the projection pattern of their axons (data not shown).

We then hypothesized that *Hrlim* may be involved in regulating the common properties in all three types of motor neurons, since *Hrlim* is expressed in all of their precursor cells. One such common property could be the *TuNa2* ion channel gene that is predominantly expressed in motor neurons. To test this possibility, *Hrlim* was misexpressed in cells other than motor neurons and *TuNa2* expression in these cells was examined. For this purpose, the same 3.4-kb DNA fragment containing the *syt* promoter used for overexpression of GFP or *DN-TuKv2* in motor neurons was employed because it drives transient gene expression in the epidermal precursors (Katsuyama *et al.*, 2002). GFP-*Hrlim* fusion plasmids were injected into B3 blastomeres at the four-cell stage or into b4.2 blastomeres at the eight-cell stage, which gave rise to the epidermal lineages (Conklin, 1905). Figure 7B shows a typical result of such misexpression of the GFP-*Hrlim* fusion gene. GFP fluorescence was observed in nuclei of the cells in the ventral epidermis of the tail. The location of GFP signals is

FIG. 5. Double staining with anti-GFP antibody and *TuNa2*-specific riboprobe confirms that the *TuNa2* gene is expressed in all three motor neuron pairs at the larval stage. (A–C) *In situ* hybridization preparations with the *TuNa2* probe before immunostaining. *TuNa2* expression was detected as dark blue signals. In some cases, the signal of *TuNa2* is weaker in Moto-*c* than in the other motor neurons. For example, in (A), *TuNa2* signal in Moto-*c* is observed only on one side of neural tube. In (B), a weak signal is detected only in the left Moto-*c*. (D–G) Larvae after whole-mount immunostaining with anti-GFP antibody. Larvae in (D), (E, F), and (G) are the same as those shown in (A), (B), and (C), respectively. Brown signals indicate GFP expression. In (D), Moto-*a* expresses GFP. The brown signal in the cell soma of Moto-*a* was not clear because it overlapped entirely with the dark blue signal of *in situ* hybridization. In a larva (E, dorsal view; F, lateral view), Moto-*b* expresses GFP. In (F), the descending axon of Moto-*b* innervates ventral muscle. In (G), Moto-*c* expresses GFP as seen from an elongated shape of the somata and its associated descending axon. Scale bar, 50 μm.

FIG. 6. Expression of *TuNa2* and *Hrlim* in putative motor neuron precursors in tailbud embryos. (A) *TuNa2* expression in the early tailbud embryo detected by whole-mount *in situ* hybridization. Two spots of *TuNa2*-positive signal (AS, anterior spot; and PS, posterior spot) are observed on each side of the neural tube. (B) A confocal optical section of *in situ* hybridization specimen just after immersing in BB/BA solution. Nuclei were stained with PI before BB/BA treatment. Initially, the dark blue dye of the *in situ* hybridization masks the PI stain in the *TuNa2*-positive spots (red arrow heads). (C) An optical section from the same embryo after the dark blue *in situ* hybridization signals have faded with time, from their solubility in BB/BA. Two nuclei (red arrows) are detected in the region corresponding to the anterior signal (red arrows). In the posterior spot (red arrow head), only one nucleus is detected. The *in situ* hybridization signal remains in the nuclei. The cells constituting the anterior spot are small and flat; the cell of the posterior spot (corresponding to Moto-*c* precursor) is large, nearly oval in shape and positioned slightly ventral to the other two cells. (D, G) Whole-mount *in situ* hybridization with *Hrlim* probe. (D) Early tailbud embryo. Two spots of *Hrlim*-positive signal are observed on each side of the neural tube. The posterior signal was weaker than the anterior signal in contrast with TuNa2 in which the two spots were equally intense. (G) *Hrlim* signals in a midtailbud embryo. Only the anterior pair of spots is observed; the posterior signal has disappeared by this stage. (E, F ,H ,I) Confocal images of PI-stained embryos before (E, H) and after (F, I) signals of *in situ* hybridization had faded. In the early tailbud embryo (E, F), two cells constitute the anterior spot (arrows in F), and one cell is included in the posterior spot (small arrowhead in E and F). Larger arrowhead in (E) shows the anterior spot. The picture in (F) shows patterns similar to those of *TuNa2* expression at this stage. In the midtailbud stage (H, I), two cells (arrows in I) express *Hrlim* (AS in G, and arrowhead in H). At this stage, no signal is seen in the corresponding region of the posterior spot (PS in D) of earlier embryos. Scale bar, 100 μm.

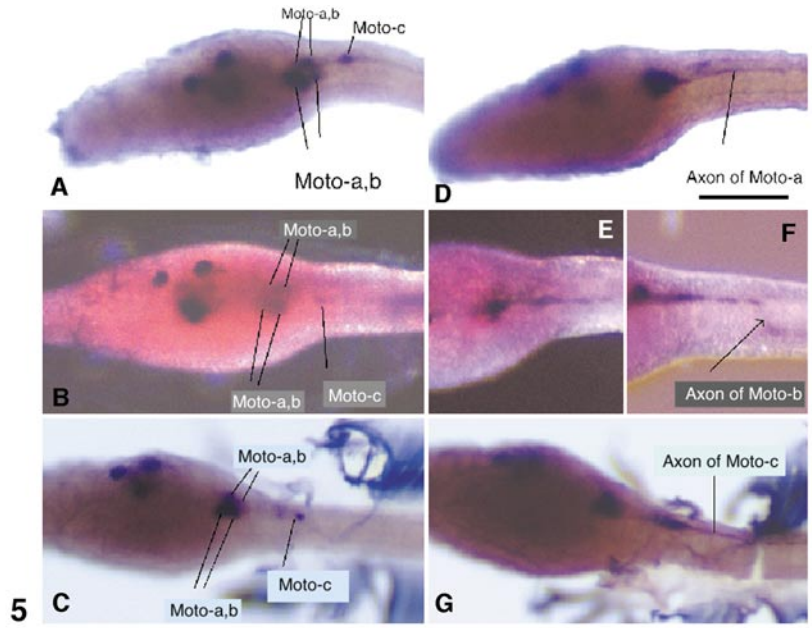

5

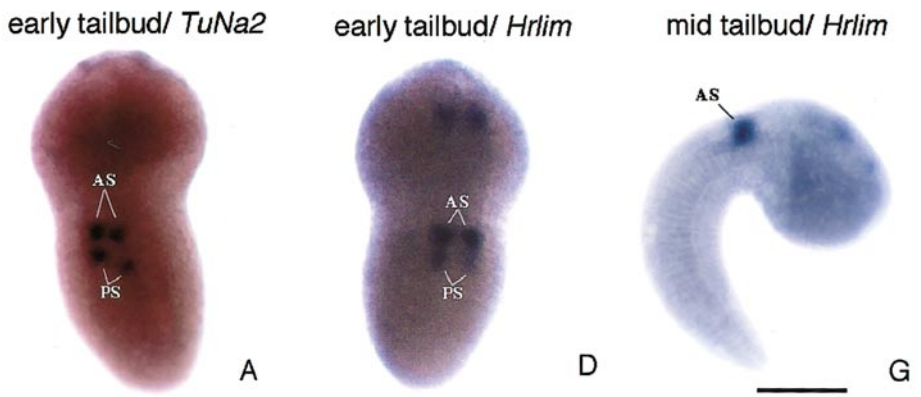

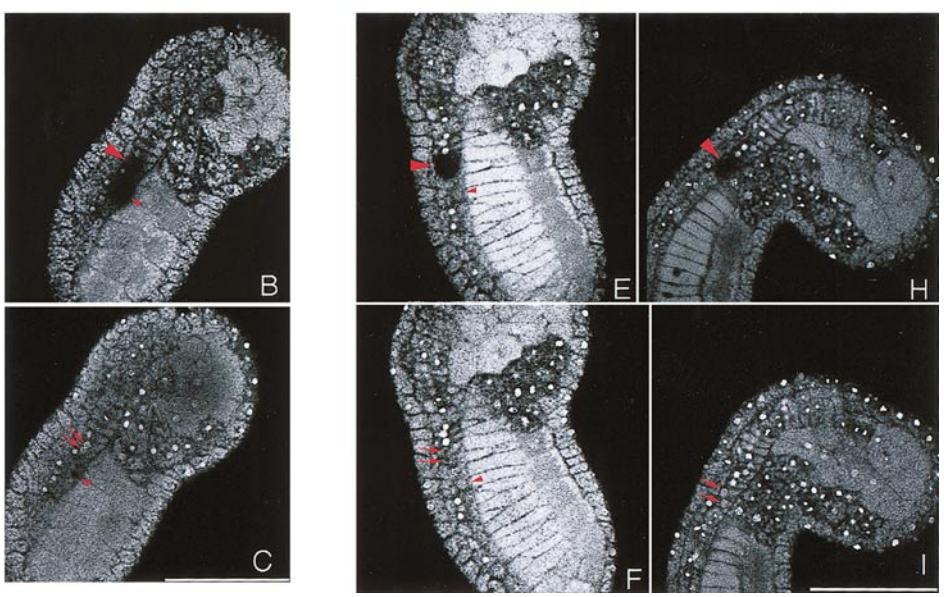

6

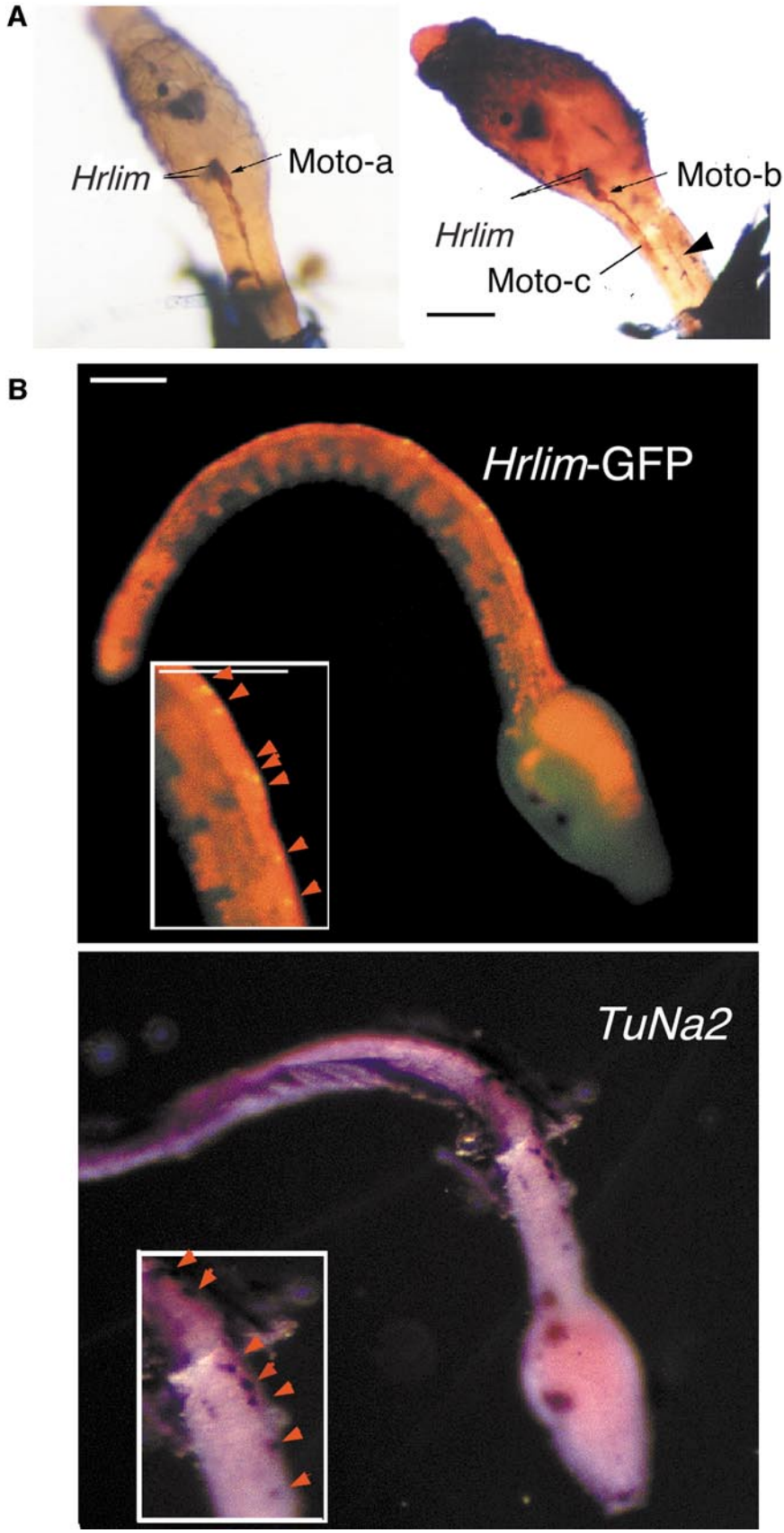

clearly distinct from the distribution pattern of epidermal sensory neurons (Ohtsuka *et al.*, 2000) that are also derived from B3. This result indicates that cells ectopically expressing *Hrlim* are epidermal cells. These larvae were processed for whole-mount *in situ* hybridization with the *TuNa2* probe. Ectopic expression of *TuNa2* appeared in the same region as for the GFP-*Hrlim* fusion protein (Fig. 7B). During the incubation for staining, ectopic *TuNa2* signals were detected earlier than endogenous *TuNa2* signals in the motor neurons, suggesting that ectopic expression of the *TuNa2* transcripts in the epidermal cells was robust. As a negative control, truncated *Hrlim* was misexpressed in the epidermal lineage. In such larvae, ectopic induction of the *TuNa2* gene expression could not be detected (data not shown). In contrast to the *TuNa2* gene, *TuNa1* and the *syt* gene that are expressed pan-neuronally could not be activated by ectopic expression of *Hrlim* in the epidermal cells (data not shown).

DISCUSSION

Diversity of Larval Motor Neurons and Their Control of Motile Behavior

In this study, we identified three pairs of motor neurons in the CNS of *H. roretzi* larvae and their progenitors in the neural tube by expressing GFP under the control of the *syt* promoter. Each of the three types of motor neurons showed a unique position, morphology, and innervation pattern in the muscle bands: Moto-*a* and Moto-*c* extended their axons towards the dorsal muscles, whereas Moto-*b* extended its neurite toward the ventral muscles.

The three pairs of motor neurons are derived from the A5.2 blastomere of the 16-cell-stage embryo and are likely to be the only population of functional motor neurons. As shown in our previous work (Okada *et al.*, 1997), the a4.2 or b4.2 blastomeres that contain cell fate in the neural tube do not give rise to any neurites in the tail, a fact which suggests that these two lineages do not contribute to any motor neuron. In *Molgula*, however, it was previously shown that some neurons, posterior to the sensory vesicle, extend neurites toward muscle cells, a fact which raises the possibility that these neurons could also be motor neurons (Vorontsova *et al.*, 1997). We found that some neurons in the posterior region of the sensory vesicle originated from the A5.1 blastomere. However, A5.1-derived neurons did not extend neurites to the muscle, at least at the level detectable by a light microscope. In addition, when a dominant negative K^+ channel gene was introduced into A5.2-derived neurons, complete paralysis was caused on the injected side. These findings provide evidence that motor neurons are exclusively derived from A5.2 in *Halocynthia* larvae. The localization and cell lineage of three motor neurons in the larva of *Halocynthia* are also consistent with the cellular organization of the visceral ganglion in the larva of *Ciona*, but in *Ciona* there are five pairs of motor neurons (Stanley-MacIsaac, 1999).

Considering that muscle cells of ascidian larvae are connected electrically with each other by means of gap junctions (Katz, 1983; Bone, 1992), synaptic input from one motor neuron could give rise to Ca^{2+} action potentials that spread all over the muscles on one side of the tail. In fact, action potentials evoked by proximal synaptic input propagate along the muscle from anterior to posterior (Bone, 1992). On the other hand, dorsal axons of *Halocynthia* larvae run along dorsal muscles to a point near the tip of tail (for example, see Figs. 2B and 2C). This pattern suggests that dorsal axons make multiple synapses on dorsal muscles throughout tail. Furthermore, ventral axons make synapses on ventral muscles in *Halocynthia* larvae (Okada *et al.*, 1997). Such an innervation pattern has also been reported in other species of ascidians (Bone, 1992; Vorontsova *et al.*, 1997). Why then does the ascidian larva need multiple inputs on each side of its tail, and what is the functional significance of ventral innervation by Moto-*b*?

FIG. 7. (A) Detection of *Hrlim* gene expression in Moto-*a* at the larval stage by double staining by *in situ* hybridization and anti-GFP antibody. (Left) One pair of cells, Moto-*a*, express *Hrlim* (dark blue signal of alkaline phosphatase activity). Brown signal of HRP activity due to GFP expression is detected in the cell body of a Moto-*a* on the right side and its descending axon, indicating that GFP is expressed in the Moto-*a* on the right side of the caudal nerve cord. The Moto-*a* detected by GFP expression overlaps with the dark blue *Hrlim* signal. (Right) A case in which GFP is expressed in Moto-*b* and -*c*, but not in Moto-*a*. GFP expression in Moto-*b* is indicated by the presence of a ventral axon (arrowhead). The brown signal due to the expression of GFP in Moto-*c* is out of focus in this picture. A pair of dark blue signals of *Hrlim* is positioned anterior to the soma of Moto-*b* (arrow), which shows brown signal. This indicates that *Hrlim* is expressed only in Moto-*a*. Scale bar, 100 μm. (B) Ectopic *TuNa2* expression induced by the misexpression of *Hrlim* in the epidermis. The GFP-*Hrlim* fusion construct under the *syt* promoter was microinjected into the *B3* blastomere at the four-cell stage. (Top) Signals of the GFP-*Hrlim* fusion protein are observed on the ventral side (top of picture) of the epidermis as yellow signals. GFP signals appear yellow, because signals of GFP overlapped with red signals of coinjected fast green. GFP signals appear as small spots in the ventral epidermis, indicating that GFP-Hrlim fusion proteins are confined to nuclei of epidermal cells. The red signal is fast green that was coinjected with DNA, confirming that DNA was inherited to descendant cells of the *B3* blastomere. (Bottom) The same embryo in the upper panel was processed to detect *TuNa2* gene expression by *in situ* hybridization. In the ventral epidermis, individual dark blue signals of *TuNa2* appear to coincide with GFP-*Hrlim* spots (as shown by insets), indicating that *TuNa2* gene expression is induced in cells expressing Hrlim protein. Signals in the trunk region indicate endogenous *TuNa2* expression as previously shown (Nagahora *et al.*, 2000). Scale bar, 100 μm.

One plausible answer to the former question might be that innervation on different tail muscle bands is in some way necessary to coordinate the high rate of flexion of the tail, 15–20 Hz in *C. intestinalis* (Bone, 1992) and 8–20 Hz in *H. roretzi* (personal communication from K. Nakajo). Synaptic input at multiple sites would help to increase the high rate of contraction of the tail muscle. Alternatively, Moto-*b* may have a role in a specific mode of behavior. *Ciona* and *Dendrodoa* tadpole larvae both show two distinct modes of movement: symmetrical movement that underlies forward swimming and tail flicks, a series of regular twitchings to one side of the tail (Bone, 1992). When the tail is truncated caudal to the ventral motor neuron fiber, the isolated tail fails to exhibit symmetrical swimming but retains movement of the tail flick (Bone, 1992). It may be possible that ventral innervation corresponds to either specific mode of movement, the symmetrical swimming or the tail flick. Future experiments such as laser ablation experiments will be necessary to clarify the physiological significance of each type of motor neuron.

Moto-*c*, the most posteriorly located neuron pair, showed several properties distinct from those of Moto-*a* or -*b*. First, Moto-*c* has a large, elongated soma, whereas Moto-*a* and -*b* have rather compact cell bodies. Second, Moto-*c* was spaced by one or two cells from Moto-*b*, whereas Moto-*a* and -*b* are located next to each other. Third, during development, Moto-*c* seems to derive from a precursor that is distinct from that of Moto-*a* and -*b* in the gastrula (Y.K., unpublished results). Fourth, temporal gene expression patterns differ between Moto-*c* and the other two motor neurons. *Hrlim* expression in the precursor of Moto-*c* started later and was down-regulated earlier than in Moto-*a* and -*b*, as shown in this study. Moto-*c* also showed a weaker *TuNa2* signal than did the other two neurons at the larval stage. Finally, it has recently been shown that a monoclonal antibody against gelsolin, originally raised against *Halocynthia* body wall muscle, also recognizes one motor neuron and its neurite in the caudal neural tube (Ohtsuka *et al.*, 2000). This cell appears to be Moto-*c*, based on its position and on the projection pattern of its neurite. The absence of gelsolin signal in the other neuronal cells in the neural tube suggests that the molecular nature of Moto-*c* is distinct from those of the other two motor neurons. One intriguing argument for such distinct properties of Moto-*c* and its spacing from the two anterior pairs of neurons is that a residual segmental organization of the neural tube could have been inherited from an ancestral chordate. Reiterated positioning of neuron clusters is one of the prominent anatomical features of the chordate neural tube. Recent cloning of the *Amphioxus Islet* gene has disclosed the segmental localization of motor neuron clusters within the region corresponding to the vertebrate hindbrain (Jackman *et al.*, 2000), suggesting that the origin of motor neuron segmental alignment predates the evolution of cephalochordates. To address this point, it will be interesting to know whether Moto-*a* and -*b* can be regarded as a neuron cluster which corresponds to one segment of the vertebrate hindbrain, and if Moto-*c* belongs to another segment.

Role of Hrlim in Motor Neuron Differentiation

We showed that *Hrlim*, a previously identified LIM-homeodomain protein gene (Wada *et al.*, 1995), is expressed in all *H. roretzi* motor neuron precursors at the early tailbud stage and is regulated in a cell-specific manner during subsequent developmental stages. It has been known that Lim class homeobox genes determine the subtype of motor neurons (Tsuchida *et al.*, 1994; Thor *et al.*, 1999). LIM-homeodomain protein participates in determining subtypes of motor neurons and their resultant projection pattern. Target specificity of motor neurons is known to be regulated by the expression pattern of complexes of multiple LIM class genes (Tsuchida *et al.*, 1994; Thor *et al.*, 1999). For example, in the mouse, *Lhx3* and *Lhx4* are shown to be expressed in motor neurons innervating ventral muscles and to determine the ventral projection of this subset of motor neurons (Sharma *et al.*, 1998). Because only Moto-*b* extends its axon toward the ventral muscle band, we first predicted that *Hrlim* expression in Moto-*b* could differ from that in the other two cells from the early tailbud stage. However, *Hrlim* expression is neither exclusive to Moto-*b*, nor spared from Moto-*b*. *Hrlim* expression is, in fact, detected in all three pairs of motor neuron precursors at the early tailbud stage. Expression in Moto-*b* coincides with that in Moto-*a* at least until the midtailbud stage, when expression in Moto-*c* is down-regulated. No change in innervation pattern was found when a homeodomain-deleted *Hrlim*, a potential dominant negative form, was overexpressed in the three motor neurons by using the *syt* promoter (data not shown). To date, therefore, it is unclear whether ventral innervation of Moto-*b* is related to *Hrlim*. The identity and target specificity of ascidian motor neurons may be determined by combinatory actions of multiple genes as in vertebrates (Tsuchida *et al.*, 1994). A test of whether motor neurons are identified by a "LIM-code" in the ascidian larva will have to await further characterization of other members of LIM class homeodomain proteins.

On the other hand, we showed that misexpression of *Hrlim* in the epidermal lineage ectopically activated the expression of *TuNa2*, a gene abundantly expressed in all motor neurons. This result leads us to interpret that Hrlim protein regulates membrane excitability of motor neuron precursors. However, in contrast to the *TuNa2* gene, the *TuNa1* gene, a voltage-gated sodium channel gene pan-neuronally expressed in both the CNS and PNS, could not be induced by ectopic expression of *Hrlim* in the epidermal lineage. Another pan-neuronally expressed gene, *syt*, coding a key protein for regulated exocytosis for synaptic transmission, was also not induced. *Hrlim* could be involved in regulating some traits specific to motor neurons. Alternatively, Hrlim needs to cooperate with other factors in inducing other phenotypes of motor neurons.

ACKNOWLEDGMENTS

We thank Drs. S. Wada and H. Saiga (Tokyo Metropolitan University) for kindly providing the *Hrlim* cDNA plasmid and Dr. I. A. Meinertzhagen (Dalhousie University) for helpful discussion and reading the manuscript. We are also grateful to Dr. H. Okamoto (AIST) for criticism on the manuscript and helpful support and Drs. Patrick Lemaire, Clare Hudson (Institut de Biologie du Développement de Marseille), and Ms. Mary E. Anderson (SUNY at Stony Brook) for critical reading. This work was partially supported by a grant of the COE program to AIST from the Agency of Science and Technology of Japan.

REFERENCES

Bone, Q. (1992). On the locomotion of ascidian tadpole larvae. *J. Mar. Biol. Ass. U. K.* **72,** 161–186.

Conklin, E. G. (1905). The organization and cell lineage of the ascidian egg. *J. Acad. Nat. Sci.* **13,** 1–119.

Edlund, T., and Jessell, T. M. (1999). Progression from extrinsic to intrinsic signaling in cell fate specification: A view from the nervous system. *Cell* **96,** 211–224.

Hikosaka, A., Kusakabe, T., Satoh, N., and Makabe, K. W. (1992). Introduction and expression of recombinant genes in ascidian embryo. *Dev. Growth Differ.* **34,** 627–634.

Hirano, T., and Nishida, H. (1997). Developmental fates of larval tissues after metamorphosis in ascidian *Halocynthia roretzi*. I. Origin of mesodermal tissues of the juvenile. *Dev. Biol.* **192,** 199–210, doi:10.1006/dbio.1997.8772.

Jackman, W. R., Langeland, J. A., and Kimmel, C. B. (2000). Islet reveals segmentation in the Amphioxus hindbrain homolog. *Dev. Biol.* **220,** 16–26, doi:10.1006/dbio.2000.9630.

Katsuyama, Y., Matsumoto, J., Okada, T., Cheng, L., Okado, H., and Okamura, Y. (2002). Regulation of synaptotagmin gene expression during ascidian embryogenesis. *Dev. Biol.* **243,** 293–304.

Katz, M. J. (1983). Comparative anatomy of the tunicate tadpole *Ciona intestinalis*. *Biol. Bull.* **164,** 1–27.

Kikuchi, Y., Segawa, H., Tokumoto, M., Tsubokawa, T., Hotta, Y., Uyemura, K., and Okamoto, H. (1997). Ocular and cerebellar defects in zebrafish induced by overexpression of the LIM domains of the islet-3 LIM/homeodomain protein. *Neuron* **18,** 369–382.

Meinertzhagen, I. A., and Okamura, Y. (2001). The larval ascidian nervous system: The chordate brain from its small beginnings. *Trends Neurosci.* **24,** 401–410.

Nagahora, H., Okada, T., Yahagi, N., Chong, J. A., Mandel, G., and Okamura, Y. (2000). Diversity of voltage-gated sodium channels in the ascidian larval nervous system. *Biochem. Biophys. Res. Commun.* **275,** 558–564, doi:10.1006/bbrc.2000.3290.

Nicol, D., and Meinertzhagen, I. A. (1988a). Development of the central nervous system of the larva of the ascidian, *Ciona intestinalis* L. I. The early lineages of the neural plate. *Dev. Biol.* **130,** 721–736.

Nicol, D., and Meinertzhagen, I. A. (1988b). Development of the central nervous system of the larva of the ascidian, *Ciona intestinalis* L. II. Neural plate morphogenesis and cell lineages during neurulation. *Dev. Biol.* **130,** 737–766.

Nicol, D., and Meinertzhagen, I. A. (1991). Cell counts and maps in the larval central nervous system of the ascidian *Ciona intestinalis* (L.). *J. Comp Neurol.* **309,** 415–429.

Nishida, H. (1987). Cell lineage analysis in ascidian embryos by intracellular injection of a tracer enzyme. III. Up to the tissue restricted stage. *Dev. Biol.* **121,** 526–541.

Nishida, H., and Satoh, N. (1985). Cell lineage analysis in ascidian embryos by intracellular injection of a tracer enzyme. II. The 16- and 32-cell stages. *Dev. Biol.* **110,** 440–454.

Ohtsuka, Y., Okamura, Y., and Obinata, T. (2000). Changes in gelsolin expression during ascidian metamorphosis. *Dev. Genes Evol.* **211,** 252–256, doi:10.1007/s004270100134.

Okada, T., Hirano, H., Takahashi, K., and Okamura, Y. (1997). Distinct neuronal lineages of the ascidian embryo revealed by expression of a sodium channel gene. *Dev. Biol.* **190,** 257–272, doi:10.1006/dbio.1997.8708.

Okamura, Y., Ono, F., Okagaki, R., Chong, J. A., and Mandel, G. (1994). Neural expression of a sodium channel gene requires cell-specific interactions. *Neuron* **13,** 937–948.

Ono, F., Katsuyama, Y., Nakajo, K., and Okamura, Y. (1999). Subfamily-specific posttranscriptional mechanism underlies K(+) channel expression in a developing neuronal blastomere. *J. Neurosci.* **19,** 6874–6886.

Satoh, N. (1994). "Developmental Biology of Ascidians." Cambridge Univ. Press, Cambridge, UK.

Sharma, K., Sheng, H. Z., Lettieri, K., Li, H., Karavanov, A., Potter, S., Westphal, H., and Pfaff, S. L. (1998). LIM homeodomain factors Lhx3 and Lhx4 assign subtype identities for motor neurons. *Cell* **95,** 817–828.

Stanley-MacIsaac, S. (1999). Ultrastructure of the visceral ganglion in the ascidian larva *Ciona intestinalis*: Cell circuitry and synaptic distribution. *Biology, Dalhousie University,* Ph.D. thesis.

Swalla, B. J., Just, M. A., Pederson, E. L., and Jeffery, W. R. (1999). A multigene locus containing the Manx and bobcat genes is required for development of chordate features in the ascidian tadpole larva. *Development* **126,** 1643–1653.

Thor, S., Andersson, S. G., Tomlinson, A., and Thomas, J. B. (1999). A LIM-homeodomain combinatorial code for motor-neuron pathway selection. *Nature* **397,** 76–80.

Tsuchida, T., Ensini, M., Morton, S. B., Baldassare, M., Edlund, T., Jessell, T. M., and Pfaff, S. L. (1994). Topographic organization of embryonic motor neurons defined by expression of LIM homeobox genes. *Cell* **79,** 957–970.

Vorontsova, M. N., Nezlin, L. P., and Meinertzhagen, I. A. (1997). Nervous system of the larva of ascidian Molgula citrina (Alder and Hancock, 1848). *Acta Zool.* **3,** 177–185.

Wada, S., Katsuyama, Y., Yasugi, S., and Saiga, H. (1995). Spatially and temporally regulated expression of the LIM class homeobox gene Hrlim suggests multiple distinct functions in development of the ascidian, *Halocynthia roretzi*. *Mech. Dev.* **51,** 115–126.

Yamada, T., Pfaff, S. L., Edlund, T., and Jessell, T. M. (1993). Control of cell pattern in the neural tube: Motor neuron induction by diffusible factors from notochord and floor plate. *Cell* **73,** 673–686.

Received for publication September 28, 2001
Revised January 14, 2002
Accepted January 14, 2002
Published online March 11, 2002